Polyhedron 97 (2015) 148–156

Contents lists available at ScienceDirect

Polyhedron

journal homepage: www.elsevier.com/locate/poly

Dinuclear and polymeric Hg(II) complexes with 1-(2-furoyl)thiourea derivatives: Their crystal structure and related properties

O. Estévez-Hernández [a,c], J. Duque [a,c], J. Rodríguez-Hernández [b], E. Reguera [c,*]

[a] Instituto de Ciencia y Tecnología de Materiales (IMRE), Universidad de La Habana, Cuba
[b] Instituto de Investigaciones en Materiales, UNAM, Ciudad Universitaria, Circuito Exterior, 04510 México DF, Mexico
[c] Centro de Investigación en Ciencia Aplicada y Tecnología de Avanzada, IPN, Legaria 694, 11500 México DF, Mexico

ARTICLE INFO

Article history:
Received 16 March 2015
Accepted 20 May 2015
Available online 27 May 2015

Keywords:
Furoylthioureas
Mercury(II) complexes
Spectroscopic characterization
Crystal structure
Simulated annealing

ABSTRACT

Dimeric and polymeric complexes bis{[(1-(2-furoyl)-3-bencyl-3-phenylthiourea-κS)chloromercury(II)]-μ-chloro} (**$HgCl_2$-FBFT**) and *catena*-poly{[(1-(2-furoyl)-3-bencylthiourea-κS)chloromercury(II)]-μ-chloro} (**$HgCl_2$-FBT**) were prepared by reaction of $HgCl_2$ with 1-(2-furoyl)-3-bencyl-3-phenylthiourea (**FBFT**) and 1-(2-furoyl)-3-bencylthiourea (**FBT**) in ethanol. Their crystal structures were solved and refined from X-ray powder diffraction data using direct space global optimization strategy (simulated annealing) followed by the Rietveld refinement. Both solids exhibit 1:1 metal:ligand stoichiometry and a distorted tetrahedral geometry for the coordination mercury centers. The mercury(II) complexes were characterized by elemental analysis, Raman, NMR and TG-DTG data. Complex **$HgCl_2$-FBFT** crystallizes in the triclinic system, space group $P\bar{1}$, while **$HgCl_2$-FBT** crystallizes in the orthorhombic system, space group *Pcnn*. In the dimeric complex **$HgCl_2$-FBFT** each Hg(II) atom is found coordinated to S atom of ligand, and to a terminal and two bridging chlorine atoms. Neighboring dimers remain together in the solid through dipolar and quadrupolar interactions. The complex **$HgCl_2$-FBT** is a polymer of mercury(II) bridged to two chlorine ions and also coordinated by terminal chlorine ion and a molecule of ligand through the S atom. This compound exhibits intramolecular and intermolecular hydrogen bonds; these last ones are responsible for packing of the polymeric chains in a 3D framework. The photoluminescence properties indicate that both complexes are fluorescent materials with maximum emission at 425 nm.

1. Introduction

The coordination and structural chemistry of mercury(II) halides with a variety of donor atoms have attracted considerable attention due the known coordination interaction of this cation with biological molecules [1–4]. In neutral mercury halides, mercury(II) is a typical soft Lewis acid which forms strong bonds of covalent character to soft donor atoms. Mercury(II) halides generally form 1:1 (dimeric species usually) or 1:2 (often discrete monomeric molecules) complexes with neutral nitrogen, phosphorus and sulfur donor ligands depending on the molar ratio and order of addition of the reactants as well as donor properties of the ligands [5–32]. Nevertheless, in both types of complexes, mercury(II) exhibits a tetrahedral distorted geometry [13,29,30–33]. Acylthioureas are versatile ligands capable of binding to a wide variety of metal ions in different coordination modes to form stable complexes [34–40]. Coordination chemistry of such derivatives is more varied due conformational isomerism, steric effects, presence of donor sites on the substituent groups and intramolecular interactions [40–42]. Mercuric ion is highly toxic to living organisms [2,43]. Therefore, the environmental consequences of this fact have sustained interest in the chelation of mercury with sulfur containing ligands such as aroylthioureas [10,29,33]. The crystal structure of these complexes is also important for applications in coordination chemistry and bioinorganic chemistry because of the different binding features observed [5–33]. For those materials for which it is complicated to grow single crystals, crystal structure solution of molecular solids can nowadays be achieved from powder X-ray diffraction (XRD) data combined with suitable software that applies Monte-Carlo/simulated annealing strategies [44–48].

Following on our interest in the coordination chemistry of thiourea derivatives with d^{10} metal ions we have extended the structural study from XRD data; Raman, NMR, photoluminescent spectra and thermal behavior for Hg(II) complexes with two 1-(2-furoyl)thiourea derivatives 3-monosubstituted and 3,3-disusbstituted.

* Corresponding author. Tel./fax: +52 55 53954147.
E-mail address: edilso.reguera@gmail.com (E. Reguera).

http://dx.doi.org/10.1016/j.poly.2015.05.028
0277-5387/

2. Experimental

2.1. Synthesis of ligands and complexes

The 1-(2-furoyl)thiourea derivatives and complexes were synthesized as previously reported [49,50]. Briefly, the complexes are formed when ethanolic solutions (25 mL) of the involved thiourea derivative (1 mmol) and mercury(II) chloride (1 mmol, 0.272 g) are mixed under stirring at room temperature in 1:1 M ratio. The reactive mixture was left to evaporate until complex precipitates. The formed precipitates were collected by filtration, then washed with ethanol and finally air dried. Due to the insolubility of the complexes in most of the common solvents employed, we failed to crystallize the materials as single crystals, rather than polycrystalline powders. A possible future solution to our inability to grow single-crystals is the use of a very interesting reaction/crystallization apparatus recently reported [51,52]. Nevertheless, we believe that the structural study reported in this study is highly reliable and supported from spectroscopic data. Some of the synthetic and spectroscopic data for both complexes were already published [50].

Bis{[(1-(2-furoyl)-3-bencyl-3-phenylthiourea-κS)chloromercury(II)]-μ-chloro} (**$HgCl_2$-FBFT**). Yield (60%). Elem. *Anal.* Calc. for $HgCl_2C_{19}H_{16}N_2O_2S$: C, 37.50; H, 2.63; N, 4.60; S, 5.26; Hg, 33.0. Found: C, 36.84; H, 2.99; N, 4.64; S, 5.27; Hg, 37.7 [50]. Melting point (°C): 142–143 [50]. *Catena*-poly{[(1-(2-furoyl)-3-bencylthiourea-κS)chloromercury(II)]-μ-chloro} (**$HgCl_2$-FBT**). Yield (79%). Elem. *Anal.* Calc. for $HgCl_2C_{13}H_{12}N_2O_2S$: C, 29.33; H, 2.25; N, 5.26; S, 6.02; Hg, 37.7. Found: C, 29.76; H, 2.39; N, 5.47; S, 6.26; Hg, 40.1 [50]. Melting point (°C): 138–139 [50]. The observed difference between the experimental and expected values of Hg content for the two complexes was ascribed to an analysis error related to the sample preparation for ICP spectroscopy.

2.2. Measurements

Elemental analyses were performed with a Leco automatic analyzer CHNS 932 model. ICP mercury analyses were carried out with a plasma spectrometer Iris Intrepid from Thermo Elemental. Raman spectra were collected on an EZRaman-N (Enwave Optronics) Raman analyzer coupled to a Leica DM300 microscope with a 100× objective, using an excitation laser source of 905 nm wavelength and 30 mW of output power. ^1H and ^{13}C NMR spectra were recorded in $CDCl_3$ (Aldrich) on a Bruker Ascend-400 spectrometer using TMS as an internal reference. Diffused reflectance spectra were recorded in the 200–800 nm wavelength range using a Cary-5E Varian spectrophotometer. Fluorescence spectra were recorded using a FLUOROMAX-4 spectrofluorometer from HORIBA Jobin Yvon at excitation wavelength of 310 nm. TG curves were collected from 25 up to 700 °C, under nitrogen flow at a constant rate of 10° per min using a TA instrument thermobalance TGA-Q-5000 model. X-ray powder diffraction data was collected with a Bruker D8 Advanced diffractometer, equipped with a Lynxeye detector and CuKα1 radiation (1.54056 Å) at 25 °C.

2.3. X-ray diffraction data collection and structural analysis

The samples were ground using agate pestle and mortar, and mounted in a top-loaded sample holder. X-ray powder diffraction data were recorded by a linear position-sensitive Lynxeye detector with a step size (2θ) of 0.092° and a counting time of 3 s per step over an angular range of $5.0° < 2\theta < 60.0°$ using the Bragg–Brentano geometry. Indexing and subsequent refinement of lattice parameters of **$HgCl_2$-FBFT** and **$HgCl_2$-FBT** carried out using the DICVOL06 software [53] indicated a triclinic unit cell with $a = 12.1597(4)$, $b = 10.3625(3)$, $c = 9.8498(3)$ Å, $\alpha = 59.816(3)°$, $\beta = 98.794(2)°$, $\gamma = 106.667(2)°$ for **$HgCl_2$-FBFT** and an orthorhombic unit cell with $a = 21.4421(2)$, $b = 19.9504(7)$, $c = 7.5497(2)$ Å, $\beta = 90°$ for **$HgCl_2$-FBT**. The first 25 peaks were individually fit. The figure of merits for **$HgCl_2$-FBFT** and **$HgCl_2$-FBT** were $M(20) = 40$, $F(20) = 97$ and $M(28) = 40$, $F(20) = 59$, respectively. Space groups $P\,c\,c\,n$ for **$HgCl_2$-FBT** and $P\bar{1}$ for **$HgCl_2$-FBFT** were determined on the basis of systematic absences. These space groups were chosen for subsequent structure determination. The full pattern decomposition was performed with EXPO2009 [54] following the Le Bail [55] algorithm and using a split type pseudo-Voigt peak profile function [56]. The first attempts of refinement were carried out using the crystal structure reported for both 1-(2-furoyl)thiourea derivatives available from the IUCr electronic archives (References XU2401 and BQ2112). In order to check the consistency of the results obtained for space group choice, unit-cell parameters, bond distances, angles and torsions, the PLATON software program was used [57]. Fullprof [58] software program and its graphical user interface, were then employed to perform a Rietveld refinement. Having obtained the unit-cell parameters, as well as the profile terms, which were not allowed to vary during the initial Rietveld refinement cycles, bond distances and angles were restrained during the Rietveld refinement. Final Rietveld refinement converged to $R_p = 3.87$, $R_{wp} = 6.48$ for **$HgCl_2$-FBFT** (591 reflections) and to $R_p = 3.80$, $R_{wp} = 8.90$ for **$HgCl_2$-FBT** (452 reflections), respectively.

The deviation of the coordination polyhedron around the mercury atom from the ideal tetrahedral geometry was analyzed by the values for τ_4 and τ'_4 parameters [33]. For an ideal tetrahedral geometry, the value of these parameters is 1, and it is 0 for a square planar coordination, and for a distorted tetrahedron τ_4 (τ'_4) < 1. The index τ'_4 ($\tau'_4 \leqslant \tau_4$) has been proposed as a better indicator for the shape of the coordination tetrahedron [33].

To the intermolecular interactions in the solid, electrostatic forces could be contributing. From this fact, the dipole and quadrupole moments for the furoyl and benzene fragments in the considered ligands were calculated using Gaussian 09 software with DFT method using B3LYP functional and 6–21 g+(d,p) base.

3. Results and discussion

3.1. Crystal structure description

3.1.1. Crystal structure description for *$HgCl_2$-FBFT*

The XRD patterns (experimental and calculated) of compounds **$HgCl_2$-FBFT** and **$HgCl_2$-FBT** are shown in Fig. 1. Relevant crystallographic data of these solids are summarized in Table 1.

The X-ray diffraction analysis reveals that the solids under study exhibit very different molecular structures. Their patterns were indexed with triclinic (**$HgCl_2$-FBFT**) and orthorhombic (**$HgCl_2$-FBT**) unit cell. The structural models to be refined were obtained using a global optimization procedure in the direct space (simulated annealing) from an initially proposed asymmetric unit. The structures of these compounds were determined in the $P\bar{1}$ and *Pccn* space group, accommodating two and eight formula units in the unit cell for **$HgCl_2$-FBFT** and **$HgCl_2$-FBT**, respectively. The difference between the experimental and calculated patterns, from the refined crystal structures is consistent with the high figures of merit found from the crystal structures refinement process. An excellent matching of the experimental and calculated XRD patterns was observed. Fig. 2 shows the molecular structure of **$HgCl_2$-FBFT** together with the atomic labeling scheme. The refined atomic positions, the calculated interatomic distance and bond angles, and the occupation and isotropic thermal factors are available from Supplementary information. This structural information

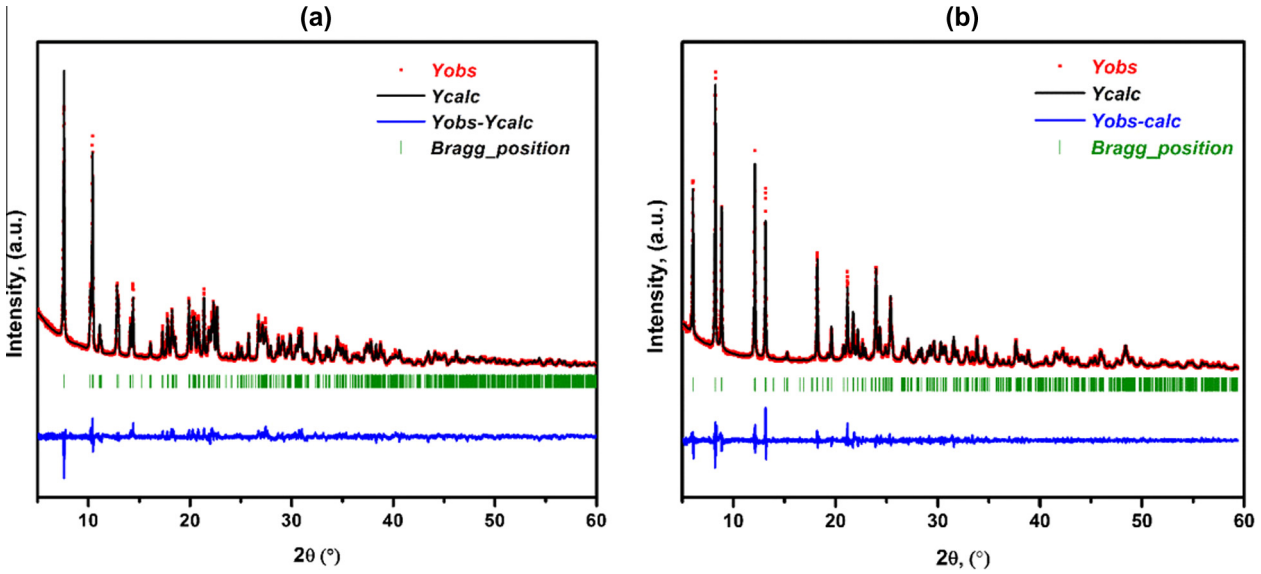

Fig. 1. Final Rietveld plot for **$HgCl_2$-FBFT** (a) and **$HgCl_2$-FBT** (b). Red curve: observed pattern; black curve: calculated pattern; blue curve: difference curve; green markers: Bragg positions for the refined structural models. (Color online.)

Table 1
Crystal data and Rietveld refinement parameters for the complexes **$HgCl_2$-FBFT** and **$HgCl_2$-FBT**.

	$HgCl_2$-FBFT	**$HgCl_2$-FBT**
Chemical formula	$HgCl_2C_{19}H_{16}N_2O_2S$	$HgCl_2C_{13}H_{12}N_2O_2S$
Formula weight (M_r)	607.91	531.81
Crystal system, space group	Triclinic, $P\bar{1}$	Orthorhombic, *Pcnn*
T (°K)	294 K	294 K
Unit cell dimensions		
a, b, c (Å)	12.1597(4), 10.3625(3), 9.8498(3)	21.4421(7), 19.9504(7), 7.5497(2)
α, β, γ (°)	59.816(2), 98.794(2), 106.667(3)	90.0000
V (Å^3)	1027.72(5)	3229.58(19)
Z	2	8
λ (Å)	1.54056	1.54056
D_{calc} (g cm^{-3})	1.960	2.188
2θ interval (°)	5.000–60.000	5.000–60.000
Step size (°), time (s)	0.092, 3	0.092, 3
No. of reflections	591	452
R_p	3.87	3.78
R_{wp}	6.48	8.89
S	1.82	2.35

was also deposited at Cambridge Structural Data Base with the CCDC file numbers indicated below. Relevant bond distances and angles are summarized in Table 2.

The complex is binuclear (dimeric) consisting of two (FBFT-Hg-Cl) moieties bridged by two chlorine atoms (Fig. 3). The mercury(II) centers are bound to S atoms ([Hg1–S1: 2.45(7) Å] of **FBFT**, a terminal chlorine atom [Hg1–Cl1: 2.69(5) Å] and the two bridging chlorine atoms [Hg1–Cl2: 2.60(5) Å], adopting a distorted tetrahedral geometry. Three of the six bond angles show significant distortion from tetrahedral geometry. The Cl2–Hg1–S1 angle has a value of 138.8(2)°, which is much larger than the tetrahedral value of 109.5°. This high angle is counter balanced by the bond angles Cl1′–Hg1–S1 and Cl1–Hg1–Cl1′, whose values are 91.14(2)° and 92.68(2)°, respectively. The two Hg and the two bridging Cl atoms are forming a square arrangement [angles: 92.68(2) and 87.32(2)° for Cl1–Hg1–Cl1′ and Hg1–Cl1–Hg1′, respectively]. Similar coordination geometries have been observed for mercury(II) complexes with N-benzoyl-N′-(2-hydroxyethyl)thiourea and N-(diethylaminothiocarbonyl) benzimido-O-methyl ester [29,59]. All bond

Table 2
Relevant bond length (in Å) and bond angle (in °) for **$HgCl_2$-FBFT**.

Bond length (Å)		Bond angle (°)	
Hg1–Cl1	2.69(5)	Cl1–Hg1–S1	110.3(2)
Hg1–Cl2	2.60(5)	Cl1′–Hg1–S1	91.14(2)
Hg1–S1	2.45(7)	Cl1′–Hg1–Cl1	92.68(2)
C2–S1	1.67(3)	Cl2–Hg1–S1	138.8(2)
		Cl2–Hg1–Cl1	103.7(2)
		Cl2–Hg1–Cl1′	109.32(2)
		Hg1–Cl1–Hg1′	87.32(2)

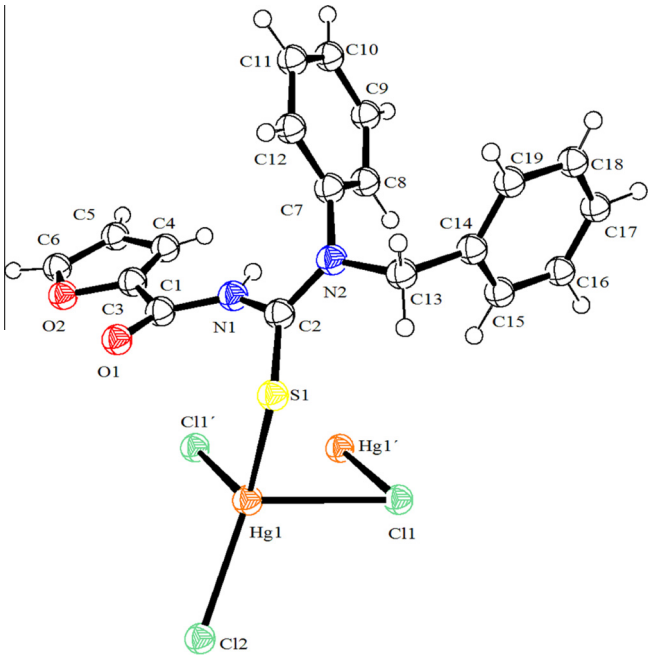

Fig. 2. A view of the molecular structure for **$HgCl_2$-FBFT**, showing the atomic numbering scheme and the thermal displacement ellipsoids drawn at the 50% probability level.

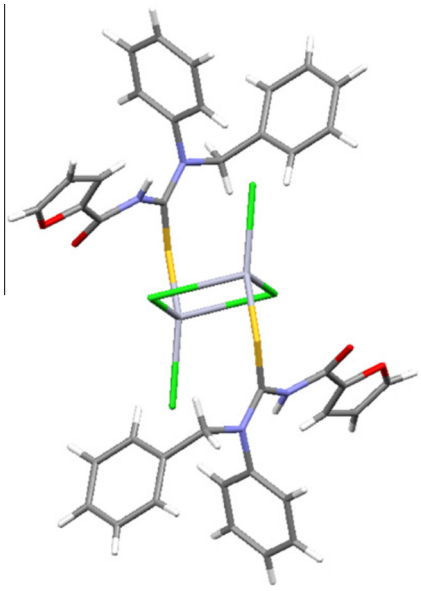

Fig. 3. Dimeric complex structure of **$HgCl_2$-FBFT**.

lengths and bond angles in **$HgCl_2$-FBFT** are in the range of expected values. On a metal coordination at S atom of a thiourea derivative, a charge transfer from the ligand to the metal must be observed reducing the double bond character of the C=S bond. For complex **$HgCl_2$-FBFT**, the C2–S1 bond distance 1.67(3) Å is longer than the C2–S1 bond distance 1.6586(16) Å in the free **FBFT** ligand [60]. From the bond angles obtained, the values for the parameters τ_4 and τ'_4 were calculated, resulting 0.79 and 0.69, respectively. This corresponds to a significant deviation from the ideal tetrahedral coordination around the Hg atom.

The **FBFT** ligand is a polar and quadrupolar molecule. It has an asymmetric charge distribution. The calculated dipolar moment for the furoyl fragment results 2.36 D, a relatively large value, compared with the one reported for the water molecule (1.85 D), for instance [61]. In the **$HgCl_2$-FBFT** complex, the furoyl fragments of neighboring dimers have an antiparallel orientation, corresponding to a dipole–dipole coupling of attractive nature (Fig. 4). Such dipolar interaction provides the force that maintains the dimers together in the solid. According to the observed ring–ring configuration, certain quadrupole–quadrupole interaction could also be present in the solid between the furoyl and benzene fragments from neighboring dimers, which are found with a quasi T-shaped configuration. The T-shaped configuration is typical for the interaction between benzene molecules related to their large negative quadrupole moment, in D, Å units, $Q_{xx} = -32.2444$; $Q_{yy} = -32.2460$; $Q_{zz} = -40.3468$ [62]. For the furoyl fragment, the calculated quadrupole moment results: $Q_{xx} = -41.2681$; $Q_{yy} = -43.2833$; $Q_{zz} = -49.1985$. Such large negative values for the quadrupole moments of these two molecular fragments explain the observed quasi T-shaped disposition between them in the crystal structure for the **$HgCl_2$-FBFT** complex (Fig. 4), with a ring-ring distance of 4.90(1) Å and a deviation of 15.5(3)° from the pure T-shaped configuration. The benzene fragments from neighboring fragments are found with a parallel stacking but the distance between them is 7.63(2) Å, quite large to be able a π–π interaction.

3.1.2. Crystal structure description for *$HgCl_2$-FBT*

Fig. 5 shows the ORTEP diagram for **$HgCl_2$-FBT** complex with the atomic numbering scheme. Details on the XRD data collection and structural refinement for this complex are summarized in Table 1. The refined atomic positions, the calculated interatomic distance and bond angles, and the occupation and isotropic thermal factors are available from Supplementary information. This structural information was also deposited at Cambridge Structural Data Base with the CCDC file numbers indicated below. Relevant bond distances and angles are summarized in Table 3. In the crystallographic asymmetric unit of this complex, the metal center is coordinated to three chloride anions and one **FBT** molecule through the sulfur atom in a distorted tetrahedral geometry. For this complex the values for the parameters τ_4 and τ'_4, result 0.84 and 0.73, respectively, which corresponds to a significant deviation from the ideal tetrahedral coordination around the Hg atom in the **$HgCl_2$-FBT** complex. For an analog complex with iodide anions, a higher distortion for the coordination geometry was reported ($\tau_4 = 0.71$, $\tau'_4 = 0.67$) [33]. Such behavior could be ascribed to a larger size for I atom.

The structure of the complex (Fig.6) may be considered as a polymer of mercury(II) bridged by the Cl1 ions [Hg1–Cl1; 2.7(3) Å] and also coordinated by terminal Cl2 ions [Hg1–Cl2;

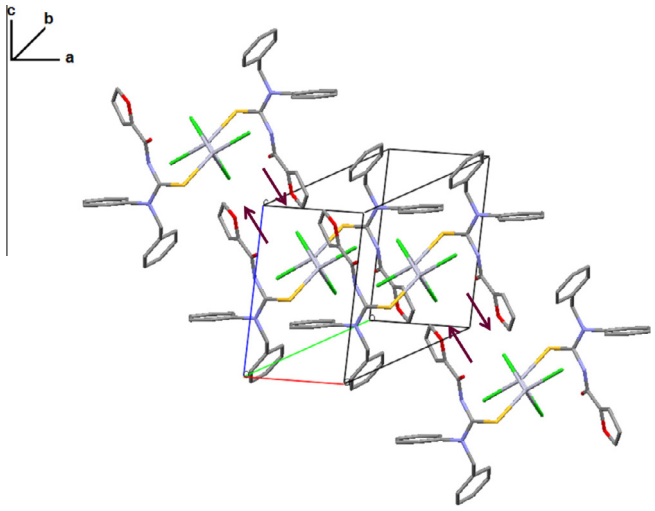

Fig. 4. Three-dimensional crystal packing in **$HgCl_2$-FBFT**. Hydrogen atoms are omitted for clarity. The opposite arrows indicate the dipole–dipole coupling between neighboring dimers.

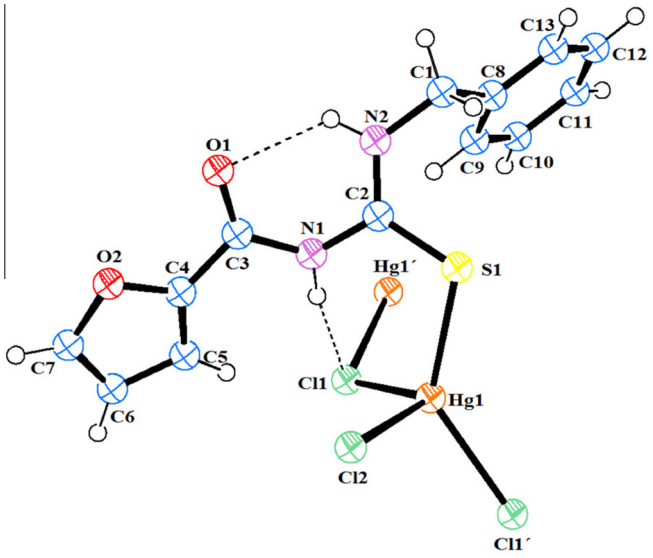

Fig. 5. A view of the molecular structure of **$HgCl_2$-FBT**, showing the atomic numbering scheme and the thermal displacement ellipsoids drawn at the 50% probability level. Selected hydrogen bonds are denoted with dashed lines.

Table 3
Relevant bond length (in Å) and bond angle (in °) for **$HgCl_2$-FBT**.

Bond length (Å)		Bond angle (°)	
Hg1–Cl1	2.7(3)	Cl1–Hg1–S1	104(7)
		Cl1′–Hg1–S1	134(2)
Hg1–Cl2	1.9(2)	Cl2–Hg1–S1	104(7)
		Cl2–Hg1–Cl1′	102(3)
Hg1–S1	2.5(4)	Cl1–Hg1–Cl2	109(9)
		Cl1′–Hg1–Cl1	113(2)
C2–S1	1.7(4)		

1.9(2) Å] and a molecule of ligand [Hg1–S1; 2.5(4) Å]. **FBT** molecules adopt the typical pseudo-*S*(6) planar ring via intramolecular hydrogen bond N2-H···O1. This hydrogen bond is bifurcated and centrosymmetric dimer is formed (Fig. 7). Additionally there is an intramolecular hydrogen bond N1-H···Cl1 (Fig. 5). Parameters for both hydrogen bonds are summarized in Table 4. A very similar coordination pattern to **$HgCl_2$-FBT** has been recently reported for a mercury(II) complex with 1-benzoyl-3-(2-methylphenyl)thiourea [33]. The C2-S1 bond distance of 1.7(4) is longer compared to an earlier reported value [63] of 1.679(2), showing strong Hg-S bonding. The Hg-S distance is in the range expected for Hg-S bonding [33,64]. The bonding parameters within the **FBT** ligand agree with those of other thiourea derivatives complexes of Hg(II) [13,29,33].

Fig. 8 shows the packing of polymer chains. Such 3D packing is possible through the network of intermolecular hydrogen bond bridges (Fig. 7), and also by de dipolar interaction between chains (discussed below). The centrosymmetric dimer formation gives additional stabilization energy to the crystal structure of **$HgCl_2$-FBT**. The benzene and furoyl fragments from neighboring **FBT** molecules, distant at 6.59(3) Å, are found with a large deviation of 64.8(5)° from the T-shaped configuration observed for the **$HgCl_2$-FBFT** complex, which was ascribed to practically absence of quadrupole–quadrupole interaction between them. The furan rings from neighboring molecules are found at a distance of 3.98(4) Å between them with a parallel-displaced configuration. This supposes that neighboring furoyl fragments remain strongly coupled through attractive dipole–dipole interaction, which stabilizes the observed stacking for the furan rings. Such dipolar interaction is contributing to the chains packing to form the 3D framework.

3.2. Spectroscopic data

The determination of crystal structures from XRD powder data has certain limitations when compared with the single crystal method, because the crystal model (3D) to be refined must be derived from data collected in 1D (one-dimension, the Bragg angle). By this reason, the refined crystal structure must be validated with additional physical measurements, usually from spectroscopic techniques, which also provide structural information on the material under study. For the complexes of thiourea derivatives with heavy metals, Raman and NMR spectroscopies are suitable techniques in that sense. The intensity of the Raman dispersion is determined by the polarizability of the involved atoms in the considered vibration motion and heavy metals have a high polarizable electron cloud. The charge donation to the metal on the complex formation induces a charge redistribution within the molecule, which could be sensed comparing its NMR spectra before and after complexation. The Raman and NMR spectral information discussed below is in accordance with the refined crystal structures for the two herein studied complexes.

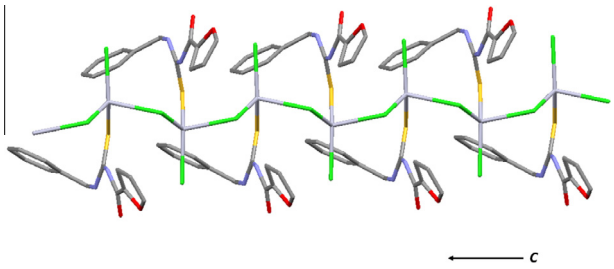

Fig. 6. Coordination polymer chain in structure of **$HgCl_2$-FBT**. Hydrogen atoms are omitted for clarity.

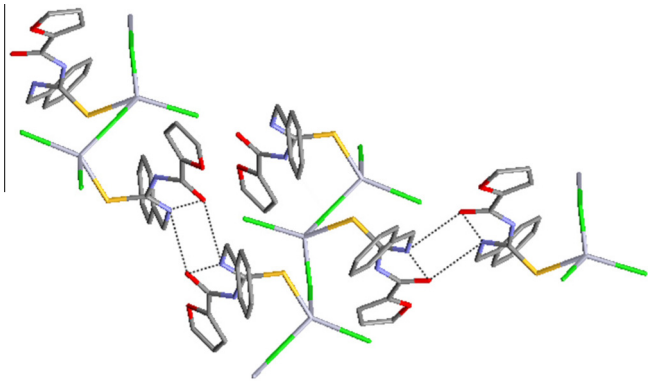

Fig. 7. Centrosymmetric dimer and bifurcated intermolecular N2-H···O1 hydrogen bonds denoted with dashed lines found in structure of **$HgCl_2$-FBT**. Hydrogen atoms are omitted for clarity.

Table 4
Hydrogen bond parameters in structure of **$HgCl_2$-FBT**.

	D–H, Å	H···A, Å	D···A, Å	D–H···A, Å
N2–H1···O1	0.88	2.24	2.80(9)	125
N1–H4···Cl2	0.88	2.06	2.8(3)	169

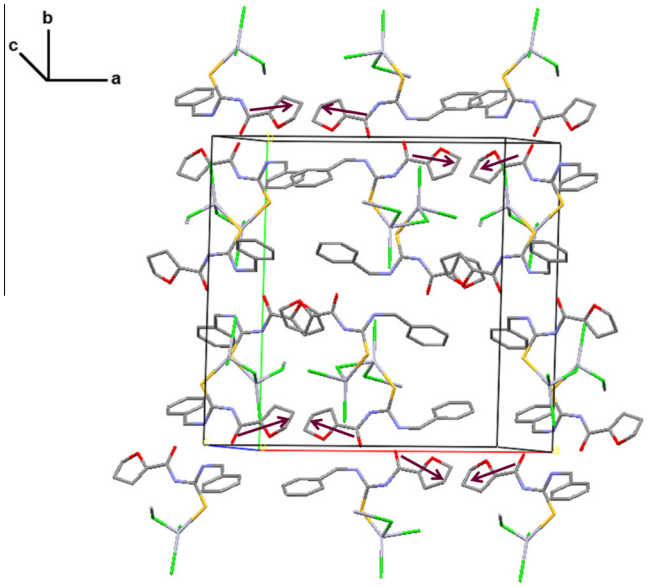

Fig. 8. Three-dimensional crystal packing in **$HgCl_2$-FBFT**. The chains packing to form a 3D framework is possible by the presence of intermolecular hydrogen bridges and dipole–dipole interactions (opposite arrows) among neighboring furoyl fragments. Hydrogen atoms are omitted for clarity.

3.2.1. Raman

The vibrational spectra of thiourea derivatives and their complexes are rich in vibrational modes with presence of many

combinations of elemental motions in the molecule. On the complex formation with metal ions, the charge redistribution within the ligand and the restrictions concerning its possible conformations, lead to changes in the vibrational spectra, both in the bands position and their relative intensity [50]. Such features are appreciated when the Raman spectra for the ligand molecules and their complexes with $HgCl_2$ herein studied are compared (Fig. 9). The main changes are observed in the 800–200 cm^{-1} spectral range dominated by combination bands, among them the Thioamide band IV, with the main contribution from ν(C=S) stretching vibration. From this fact, this band is indicative of the metal coordination at the S atom.

Fig. 9 shows the Raman spectra for **FBFT** and **FBT** ligands and their complexes with $HgCl_2$. For the ligand molecules, the ν(C=S) vibration is observed at 697 cm^{-1} (**FBFT**) and 735 cm^{-1} (**FBT**). Upon complexation, these vibrations shift to lower frequency, at 675 and 708 cm^{-1}, respectively. That negative frequency shifting corresponds to the weakening for the force constant, the bond order, for the C=S bond, related to charge donation to the Hg atom. This is in accordance with the findings on most of the thiourea complexes reported [29,30,65]. In addition to the frequency, the vibration shows a significant intensity decrease, which is also an evidence of the coordination bond formation. On the S atom bonding to the mercury atom, the C=S-metal polarizability is dominated by the heavier atom. On the coordination bond formation, in the Raman spectrum appears a strong band related to the Hg-S stretching vibration. For **$HgCl_2$-FBFT** and **$HgCl_2$-FBT** complexes, that band is observed at 269 and 276 cm^{-1}, respectively. Mercury is a heavy and highly polarizing atom, which is responsible for the high intensity observed for that stretching band.

3.2.2. ^1H and ^{13}C NMR

The charge redistribution within the molecule and the restrictions in its conformations on the complex formation are also detected in the NMR spectrum. The conformations in the thiourea derivative molecules are closely related with the formation of intra-molecular hydrogen bond bridges [66]. From these facts, the main evidences for the complex formation must be related with ^1H and ^{13}C NMR signals corresponding to the thioamide group (HNCS). Table 5 collects the relevant ^1H and ^{13}C NMR data used as indicators for the **$HgCl_2$-FBFT** and **$HgCl_2$-FBT** complexes formation. The ^1H and ^{13}C NMR chemical shift values for all the H and C atoms in the molecule are available from Supplementary information. The results (Table 5) are consistent with the structure of the complexes. In ^1H NMR spectra, the greatest complexation effect ($\Delta\delta$) was observed at the NH protons. The observed deshielding for the NH protons in **$HgCl_2$-FBT** is caused by the presence of both, inter- and intra-molecular H-bonding in the complex (Figs. 5 and 7). In the free ligand only an intramolecular H-bridges is established. The higher deshielding effect is observed for the proton involved in the inter-molecular interactions (Table 5, Fig. 7). On the other hand, upon complexation with $HgCl_2$, the ^{13}C signal for the thioamide group shifts to low δ values compared to the free ligand. In accordance with the refined crystal structure, this confirms that mercury is bonded to sulfur, since the carbon atom in the C=S fragment is the closest carbon to the complexation site. The shift is attributed to a lowering of the C=S bond order upon coordination. The ^{13}C NMR spectrum of the complex also reveals a downfield shift of the carbonyl signal around 2–3 ppm with respect to the free ligands. This is ascribed to a strong induced effect related to the metal coordination at S atom [50].

3.3. Photoluminescence properties

Aroylthioureas derivatives usually show interesting luminescent features [66,67]. The electronic properties of the transition metal ions make them particularly attractive for the preparation of luminescent complexes. A higher thermal stability for the complex, compared with the free ligand, and a variety of coordination spheres and emitting levels is also expected [66]. This contribution includes the study of the photoluminescent properties for the **$HgCl_2$-FBFT** and **$HgCl_2$-FBT** complexes, correlating them with the emission bands of the free ligands (**FBFT** and **FBT**). The UV–visible spectral curves for both, the ligands and their complexes with $HgCl_2$, in the solid state, are shown in Fig. 10a and c, respectively.

Both complexes **$HgCl_2$-FBFT** and **$HgCl_2$-FBT** display intense absorption bands centered at 274 and 268 and nm. These bands, from $n \rightarrow \pi^*$ transitions, appear in the corresponding free ligands as broad peaks centered at 290 and 303 nm. A second band of lower intensity, from $\pi \rightarrow \pi^*$ transition, is observed as a shoulder at 313 nm for **$HgCl_2$-FBT** and well defined one for **$HgCl_2$-FBFT** at 319 nm. This band shows similar behavior for the free ligands at 350 and 370 nm, respectively. After complexation, both types of absorption band exhibit a blue shift, which was ascribed to the above mentioned charge redistribution within the molecule and a higher stabilization of its n and π energy levels.

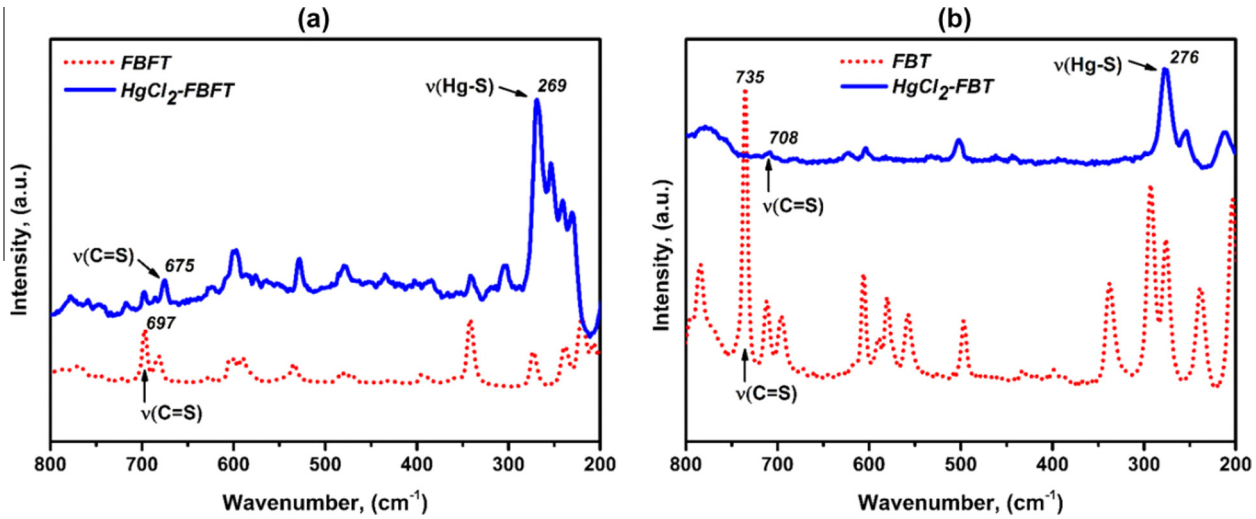

Fig. 9. (a) Raman spectra of **$HgCl_2$-FBFT/FBFT** (a) and **$HgCl_2$-FBT/FBT** (b) in the 800–200 cm^{-1} region, respectively.

Table 5
Relevant ^{1}H and ^{13}C chemical shift values, in ppm, from spectra recorded in $CdCl_3$, for the free **FBFT** and **FBT** ligands and their complexes with $HgCl_2$.

Compound	**FBFT**	**$HgCl_2$-FBFT**	Shift*, in ppm
N1–H	8.60	9.92	1.32
C2 (C=S)	178.9	177.7	1.2
C1 (C=O)	152.9	156.5	3.6
Compound	**FBT**	**$HgCl_2$-FBT**	Shift*, in ppm
N1–H	10.75	11.68	0.93
N2–H	9.17	10.44	1.27
C2 (C=S)	179.7	177.8	1.9
C3 (C=O)	156.7	158.8	2.1

* Difference of chemical shift (in ppm) between the free ligand and its complex with $HgCl_2$.

The **$HgCl_2$-FBFT** and **$HgCl_2$-FBT** complexes show broad emission bands with the maximum intensities centered at 425 nm upon excitation at 310 nm due to a ligand transition (Fig. 10b and d). The photoluminescence of the ligands has been assigned as originating from intraligand $\pi \rightarrow \pi^*$ transitions. In both cases, after complexation, the intensity of emission increases. Complex **$HgCl_2$-FBFT** show a blue shift of about 12 nm in contrast to the free ligand probably due to the quenching effect of the mercury(II) ion [32]. Complex **$HgCl_2$-FBT** show weaker emission and it is noticeable that exhibits no shift in its emission band at 425 nm. For this complex other two fluorescence bands of much lower intensity at 375 and 346 nm were observed. The violet-blue emissions of both complexes in the solid state make these materials potentially applicable in light emitting diode devices.

3.4. Thermal analyses of the complexes

In order to examine the thermal stability of the two complexes, thermogravimetric (TG) and differential thermogravimetric analyses (DTG) were carried out for compounds **$HgCl_2$-FBFT** and **$HgCl_2$-FBT** between 25 and 700 °C, under nitrogen flow (Fig. 11a and b). Complex **$HgCl_2$-FBFT** melts and simultaneously the decomposition process starts. Compared to the free ligand, the complex decomposes more slowly and at higher temperature, suggesting certain ligand stabilization. Such behavior is indicative of complex formation, in correspondence with the above discussed structural and spectroscopic study.

The thermal decomposition process is promoted by vibration of molecules and ligands induced by the thermal energy (kT), which leads to rupture of the chemical bonds involved and evolution of thermal decomposition products. For this reason, the first species to evolve are those weakly bonded or where the molecular fragment is highly sensible to the vibrational motion. The formation of a complex with mercury chloride changes the ligand vibrational pattern and, in consequence, its behavior on heating. The TGA curve indicates (Fig. 11a) that the loss of weight starts around 104 °C. The DTG curve exhibits four distinct decomposition

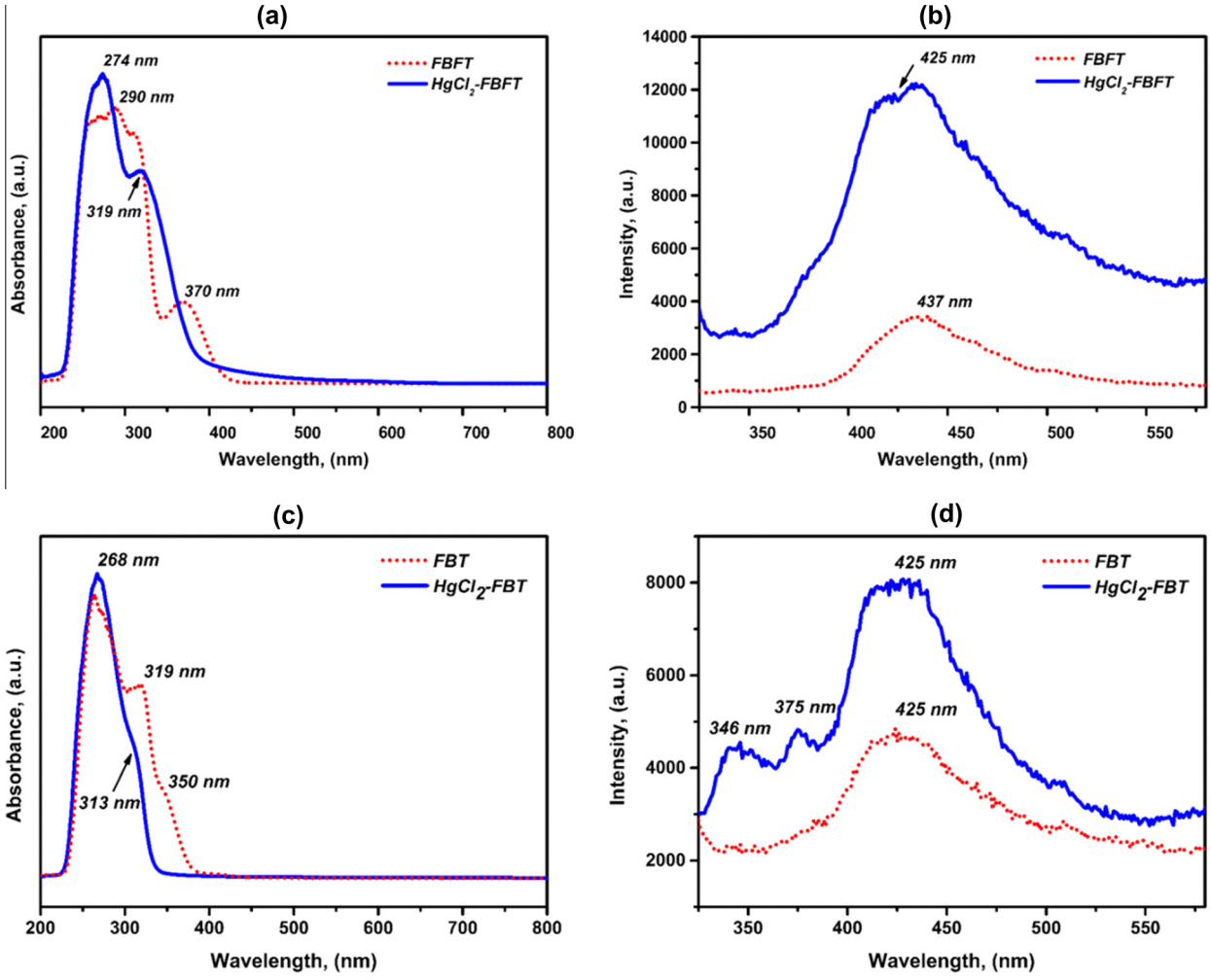

Fig. 10. UV–Vis (a,c) and emission spectra (b,d) for **$HgCl_2$-FBFT/FBFT** and **$HgCl_2$-FBT/FBT** samples, respectively.

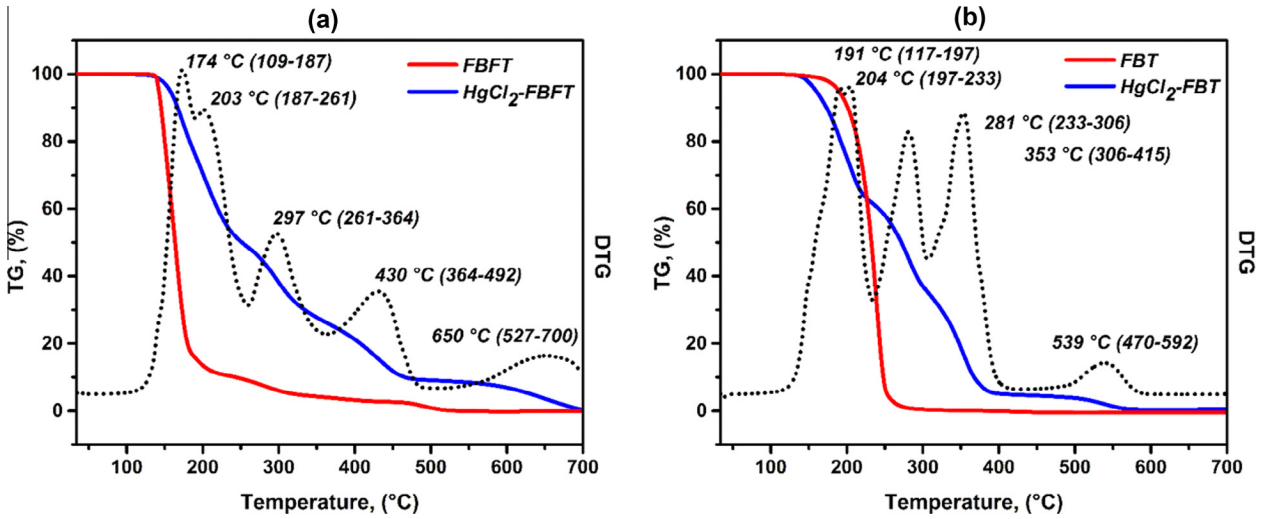

Fig. 11. TG and DTG curves showing degradation on heating for **$HgCl_2$-FBFT/FBFT** (a) and **$HgCl_2$-FBT/FBT** (b) samples, respectively.

processes centered at 190, 297, 430 and 650 °C. This behavior is quite different to that observed for the free ligand, for which the main loss of mass is produced in only one step. As discussed above, the complex **$HgCl_2$-FBFT** is binuclear with two Hg(II) ions tetrahedrally coordinated by a terminal chloride, two bridging chlorides and a FBFT molecule via S atom. The first weight loss (~50%) observed in the **$HgCl_2$-FBFT** complex centered at around 190 °C could be ascribed to the degradation of the organic moieties (except sulfur). We can expect that Hg-S links could be retained and extended (Calc.: 50.03%; Found: 49.43%). The second decomposition period takes place in 261–364 °C and it brings about 23% weight loss, probably due to the elimination of an $HgCl_2$ molecule. The percentage mass loss is close to the one expected (Calc.: 72.38%; Found: 73.16%). Finally, the two last steps are expected to be a sequential combination of dechlorination, desulfurization and evolution of metallic mercury [65]. Complex **$HgCl_2$-FBT** has polymeric structure. It melts and simultaneously the four-step decomposition process stars (Fig. 11b). Unlike what was observed for the **$HgCl_2$-FBFT** complex, in this case the solid begins to decompose at lower temperature compared to the free ligand, suggesting a weakening of bonds around the thioureide core after complexation. The first step starts around 117 °C and continues to about 233 °C at which point most of the organic part of the complex has released. It is expected that Hg-SCN linkage is maintained (Calc.: 38.00%; Found: 38.33%). The second stage of decomposition centered at 281 °C corresponds to the loss of thiocyanate [68] and chloride anions (Calc.: 62.26%; Found: 64.22%). The final steps involve evaporation of metallic mercury.

4. Conclusions

This paper reports crystal structure, spectral features, thermal behavior for mercury(II) complexes with two 1-(2-furoyl)thiourea derivatives, 3-bencyl-3-phenyl (**$HgCl_2$-FBFT**) and 3-bencyl (**$HgCl_2$-FBT**) substituted. The crystal structure, solved and refined from XRD powder data, shows a distorted four coordinate tetrahedral geometry for both compounds. Complex **$HgCl_2$-FBFT** is dimeric, involving one neutral S-monodentate **FBFT** ligand, one terminal chlorine atom and two bridging chlorine atoms around each mercury center. Neighboring dimers remain packed in a 3D structure through dipolar interactions between them. Complex **$HgCl_2$-FBT** is a coordination polymer possessing a chain structure with mercury(II) ions bridged to two chlorine ions and also coordinated by terminal chlorine ion and a molecule of ligand through the S atom. The crystal structure of this complex is stabilized by various intramolecular and intermolecular hydrogen bonding interactions; its 3D structure is supported in these last ones interactions. The recorded Raman and ^1H and ^{13}C NMR spectra support the complex formation and the refined crystal structures. Photoluminescence is associated with both complexes upon excitation at 310 nm, exhibiting a violet-blue emission at 425 nm as a consequence of intraligand $\pi \rightarrow \pi^*$ transitions. The thermal decomposition behavior appears as an indicator of the complex formation. For the complexes, it proceeds in a four-step weight loss curve with differences associated to the nature of each complex.

Acknowledgements

O.E.H. and J.D. acknowledge the financial support from Consejo Nacional de Ciencia y Tecnología (CONACyT), México, through the postdoctoral and sabbatical fellowships program (projects 233388 and 203824). This study was partially supported by the CONACyT projects 174247 and FON.INST./75/2012.

Appendix A. Supplementary data

CCDC 1015954 and 1015315 contain the supplementary crystallographic data for compounds **$HgCl_2$-FBFT** and **$HgCl_2$-FBT**. These data can be obtained free of charge via http://www.ccdc.cam.ac.uk/conts/retrieving.html, or from the Cambridge Crystallographic Data Centre, 12 Union Road, Cambridge CB2 1EZ, UK; fax: (+44) 1223 336 033; or e-mail: deposit@ccdc.cam.ac.uk. Supplementary data associated with this article can be found, in the online version, at http://dx.doi.org/10.1016/j.poly.2015.05.028.

References

[1] T.L. Blundell, J. Jenkins, Chem. Soc. Rev. 6 (1977) 139.
[2] J.R. Ashby, P.J. Craig, The Biomethylation of Heavy Metal Elements, Royal Society of Chemistry, Cambridge, 1990.
[3] D.M. Miller, J.S. Woods, Chem.-Biol. Interact. 88 (1993) 23.
[4] J.G. Wright, M.J. Natan, F.M. MacDonell, D.M. Ralston, T.V. O'Halloran, Prog. Inorg. Chem. 38 (1990) 323.
[5] N.A. Bell, S.J. Coles, C.P. Constable, D.E. Hibbs, M.B. Hursthouse, R. Mansor, E.S. Raper, C. Sammon, Inorg. Chim. Acta 323 (2001) 69.
[6] T.S. Lobana, R. Sharma, R. Sharma, R. Sultana, R.J. Butcher, Z. Anorg. Allg. Chem. 634 (2008) 718.
[7] G. Pavlović, Z. Popović, Ž. Solden, D. Matković-Čalogović, Acta Crystallogr. C56 (2000) 801.
[8] D. Matković-Čalogović, Z. Popović, G. Pavlović, Ž. Soldin, G. Giester, Acta Crystallogr. C57 (2001) 409.

[9] Z.-Y. Wu, D.-J. Xu, C.-H. Hung, J. Coord. Chem. 57 (2004) 791.
[10] M.S.M. Yusof, B.M. Yamin, M.B. Kassim, Acta Crystallogr. E60 (2004) m98.
[11] A.A. Isab, M. Fettouhi, M.R. Malik, S. Ali, A. Fazal, S. Ahmad, Russ. J. Coord. Chem. 37 (2011) 180.
[12] M.R. Malik, S. Ali, S. Ahmad, M. Altaf, H. Stoeckli-Evans, Acta Crystallogr. E66 (2010) m1060.
[13] S. Ahmad, H. Sadaf, M. Akkurt, S. Sharif, I.U. Khan, Acta Crystallogr. E65 (2009) m1191.
[14] A.A. Isab, M.I.M. Wazeer, J. Coord. Chem. 58 (2005) 529.
[15] A.A. Isab, H.P. Perzanowski, J. Coord. Chem. 21 (1990) 247.
[16] A.A. Isab, H.P. Perzanowski, Polyhedron 14 (1996) 2397.
[17] M.I.M. Wazeer, A.A. Isab, Spectrochim. Acta, Part A 68 (2007) 1207.
[18] E.S. Raper, J.R. Creighton, N.A. Bell, W. Clegg, L. Cucurull-Sanchez, Inorg. Chim. Acta 277 (1998) 14.
[19] Z. Popović, G. Pavlović, D. Matković-Čalogović, Ž. Soldin, M. Rajić, D. Vikić-Topić, D. Kovacek, Inorg. Chim. Acta 306 (2000) 142.
[20] Z. Popović, G. Pavlović, Ž. Soldin, J. Popović, D. Matković-Čalogović, M. Rajić, Eur. J. Inorg. Chem. (2002) 171.
[21] N.A. Bell, T.N. Branston, W. Clegg, J.R. Creighton, L. Cucurull-Sanchez, M.R.J. Elsegood, E.S. Raper, Inorg. Chim. Acta 303 (2000) 220.
[22] Z. Popović, D. Matkovic-Čalogović, Ž. Soldin, G. Pavlović, N. Davidović, D. Vikić-Topić, Inorg. Chim. Acta 294 (1999) 35.
[23] G. Pavlović, Z. Popović, Ž. Soldin, D. Matković-Čalogović, Acta Crystyllogr. C56 (2000) 61.
[24] Z. Popović, Ž. Soldin, G. Pavlović, D. Matković-Čalogović, D. Mrvos-Sermek, M. Rajić, Struct. Chem. 13 (2002) 425.
[25] N.A. Bell, T.N. Branston, W. Clegg, L. Parker, E.S. Raper, C. Sammon, C.P. Constable, Inorg. Chim. Acta 319 (2001) 130.
[26] F.A. Devillanova, F. Isaia, G. Verani, A. Hussein, J. Coord. Chem. 14 (1986) 249.
[27] P.L. Bellon, F. Demartin, F.A. Devillanova, F. Isaia, G. Verani, J. Coord. Chem. 18 (1988) 253.
[28] F. Cristiani, F. Demartin, F.A. Devillanova, A. Diaz, F. Isaia, G. Verani, J. Coord. Chem. 21 (1990) 137.
[29] Y.-M. Zhang, L.-Z. Yang, Q. Lin, T.-B. Wie, J. Coord. Chem. 58 (2005) 1675.
[30] M. Altaf, H. Stoeckli-Evans, S. Ahmad, A.A. Isab, A.R. Al-Arfaj, M.R. Malik, S. Ali, J. Chem. Crystallogr. 40 (2010) 1175.
[31] H. Sadaf, S. Ahmad, S. Sharif, I.U. Khan, M. Akkurt, S.W. Ng, M.I. Khan, S.A. Bashir, M. Mufakkar, J. Struct. Chem. 53 (2012) 151.
[32] A. Bharti, P. Bharti, M.K. Bharty, R.K. Dani, S. Singh, N.K. Singh, Polyhedron 54 (2013) 131.
[33] A. Okuniewski, D. Rosiak, J. Chojnacki, B. Becker, Polyhedron 90 (2015) 47. and references therein.
[34] S. Nadeem, M.K. Rauf, M. Ebihara, S.A. Tirmizi, S. Ahmad, Acta Crystallogr. E64 (2008) m698.
[35] S. Nadeem, M.K. Rauf, S. Ahmad, M. Ebihara, S.A. Tirmizi, A.B. Badshah, Transition Met. Chem. 34 (2009) 197.
[36] P. Zoufalá, T. Rüffer, H. Lang, S. Ahmad, M. Mufakkar, Anal. Sci. X-ray Struct. Anal. Online 23 (2007) x219.
[37] I.U. Khan, M. Mufakkar, S. Ahmad, H.-K. Fun, S. Chantrapromma, Acta Crystallogr. E63 (2007) m2550.
[38] M. Hanif, S. Ahmad, M. Altaf, H. Stoeckli-Evans, Acta Crystallogr. E63 (2007) m2594.
[39] A.I. Matesanz, P. Souza, J. Inorg. Biochem. 101 (2007) 1354.
[40] A. Saeed, M.F. Erben, M. Bolte, Spectrochim. Acta, Part A 102 (2013) 408.
[41] K.R. Koch, Coord. Chem. Rev. 216–217 (2001) 473.
[42] A.R. Lazo-Fraga, A. Collins, G. Forte, A. Rescifina, F. Punzo, J. Mol. Struct. 929 (2009) 174.
[43] T.W. Clarkson, Ann. Rev. Pharm. 12 (1972) 375.
[44] K. Fujii, A.L. Garay, J. Hill, E. Sbircea, Z. Pan, M. Xu, D.C. Apperly, S.L. James, K.D.M. Harris, Chem. Commun. 46 (2010) 7572.
[45] R.M. Ibberson, A.J. Fowkes, M.J. Rosseinsky, W.I.F. David, P.P. Edwards, Angew. Chem., Int. Ed. 48 (2009) 1435.
[46] U. Das, B. Chattopadhyay, M. Mukherjee, A.K. Mukherjee, Cryst. Growth Des. 12 (2012) 466.
[47] B. Chattopadhyay, S. Ghosh, S. Mondal, M. Mukherjee, A.K. Mukherjee, CrystEngComm 14 (2012) 640.
[48] O. Estévez-Hernández, J. RodríguezHernández, E. Reguera, J. Duque, J. Chem. Crystallogr. 45 (2015) 51.
[49] E. Otazo-Sánchez, L. Pérez-Marín, O. Estévez-Hernández, S. Rojas-Lima, J. Alonso-Chamarro, J. Chem. Soc., Perkin Trans. 2 (2001) 2211.
[50] O. Estévez-Hernández, E. Otazo-Sánchez, J.L. Hidalgo-Hidalgo de Cisneros, I. Naranjo-Rodríguez, E. Reguera, Spectrochim. Acta, Part A 64 (2006) 961.
[51] A.A. Khandar, B.K. Ghosh, C. Lampropoulos, M.S. Gargari, V.T. Yilmaz, K. Bhar, S.A. Hosseini-Yazdi, J.M. Cain, G. Mahmoudi, Polyhedron 85 (2015) 467.
[52] G. Mahmoudi, M.S. Gargari, F.A. Af-khami, C. Lampropoulos, M. Abedi, S.A. Corrales, A.A. Khandar, J. Mague, B.K. Ghosh, A. Masummi, Polyhedron 93 (2015) 46.
[53] A. Boultif, D. Louër, J. Appl. Crystallogr. 37 (2004) 724.
[54] A. Altomare, M. Camalli, C. Cuocci, C. Giacovazzo, A. Moliterni, R. Rizzi, J. Appl. Crystallogr. 42 (2009) 1197.
[55] A. Le Bail, H. Duroy, J.L. Fourquet, Mater. Res. Bull. 23 (1988) 447.
[56] M.M. Hall, V.G. Veeraraghvan, H. Rubin, P.G. Winchell, Appl. Crystallogr. 10 (1977) 66.
[57] A.L. Spek, Appl. Crystallogr. 36 (2003) 7.
[58] http://www.ill.eu/sites/fullprof.
[59] F. Leßmann, L. Beyer, J. Sieler, Inorg. Chem. Comm. 3 (2000) 62.
[60] O. Estévez-Hernández, R.S. Corrêa, J. Ellena, J. Duque, Acta Crystallogr. E65 (2009) o648.
[61] D.R. Lide (Ed.), CRC Handbook of Chemistry and Physics, 84th ed., CRC Press, Fl., USA, 2004.
[62] M. Gonzalez, A.A. Lemus-Santana, J. Rodríguez-Hernández, C.I. Aguirre-Velez, M. Knobel, E. Reguera, J. Solid State Chem. 204 (2013) 128.
[63] H. Pérez, Y. Mascarenhas, O. Estévez-Hernández, S. Santos Jr, J. Duque, Acta Crystallogr. E64 (2008) o695.
[64] D.L. Turner, K.H. Stone, P.W. Stephens, A. Walsh, M.P. Singh, T.P. Vaid, Inorg. Chem. 51 (2012) 370.
[65] M. Cârcu, T. Negoiu, S. Rosu, J. Serban, Therm. Anal. Cal. 61 (2000) 935.
[66] W. Zhu, W. Yang, W. Zhou, H. Liu, S. Wei, J. Fan, J. Mol. Struct. 1004 (2011) 74.
[67] C.M. Che, S.W. Lai, Coord. Chem. Rev. 249 (2005) 1296.
[68] G. Mahmoudi, A. Morsali, M. Zeller, Inorg. Chim. Acta 362 (2009) 217.